Gyrokinetic-water-bag modeling of low-frequency instabilities in a laboratory magnetized plasma column

E. Gravier, R. Klein, P. Morel, N. Besse, and P. Bertrand
*Laboratoire PMIA, UMR 7040 CNRS-Université Henri Poincaré,
F-54506 Vandoeuvre-lès-Nancy Cedex, France*

A new model is presented, named collisional-gyro-water-bag (CGWB), which describes the collisional drift waves and ion-temperature-gradient (ITG) instabilities in a plasma column. This model is based on the kinetic gyro-water-bag approach recently developed [P. Morel *et al.*, Phys. Plasmas **14**, 112109 (2007)] to investigate ion-temperature-gradient modes. In CGWB electron-neutral collisions have been introduced and are now taken into account. The model has been validated by comparing CGWB linear analysis with other models previously proposed and experimental results as well. Kinetic effects on collisional drift waves are investigated, resulting in a less effective growth rate, and the transition from collisional drift waves to ITG instability depending on the ion temperature gradient is studied. © *2008 American Institute of Physics*. [DOI: 10.1063/1.3036930]

I. INTRODUCTION

It is now widely believed that low-frequency turbulence developing from small scale instabilities is responsible for the phenomenon of anomalous transport generally observed in magnetic confinement fusion experiments.[1,2] These microinstabilities are driven by equilibrium density, ion, and electron temperature gradients. However, the physical mechanisms behind the instabilities are not yet fully understood.

Among these microinstabilities, drift waves,[3,4] ion-temperature-gradient (ITG), and trapped electron mode[2,5,6] instabilities play an important role in explaining the anomalous heat and particle transport observed in tokamaks. Indeed, edge turbulence is usually interpreted as the nonlinear saturated state of drift waves or interchange instabilities in the edge plasma.[4] In the core plasma, the main instabilities involved are the ITG driven modes and the collisionless trapped electron modes.[2]

To contribute to a better understanding of plasma instabilities, several detailed analysis were conducted in cylindrical magnetized plasmas. Typical examples are Mirabelle,[7] Mistral,[8] Kiwi,[9] Vineta,[10] the Auburn ALEXIS device (Auburn Linear Experiment for Instability),[11] or Columbia,[12] to name only a few. Low-frequency density fluctuations ($\omega \ll \omega_{Ci}$) are easily observed in linear magnetized plasma columns.

Small scale linear devices, together with numerical simulations, can play an important role in understanding basic plasma processes. To this purpose, fluid models have been widely used.[13–15] Solving three-dimensional (3D) fluid equations is the most convenient way to compute the plasma response to the perturbed electromagnetic field when there is no wave-particle interaction. Indeed, plasma phenomena observed in real experiments can be explained by a fluid model if phase velocities and thermal velocities are very different. For example, the nonlocal cylindrical model developed by Marden-Marshall and Ellis[13,14] describes how drift wave mode stability varies with azimuthal mode number in a weakly ionized plasma. For such a model, using a set of fluid equations is all the more justified because collisions constitute the usual assumption of fluid closures.

However, for some devices or for fusion plasmas, interactions between waves and particles may occur. For these experiments, it is known that the stability threshold given by fluid equations is lower than the kinetic value.[1,16] In addition, a fluid description usually overestimates turbulent fluxes. This discrepancy comes partly from the resonant interactions between waves and particles like Landau resonances, which cannot be fully described with fluid equations.

In principle, one has to solve a six-dimensional kinetic equation to determine the distribution function. However, for strongly magnetized plasmas the Larmor radius is much smaller than the characteristic density length $n/|\nabla n|$ or the characteristic magnetic field length $B/|\nabla B|$, and the cyclotron motion is faster than the turbulent one. Therefore, the Vlasov equation can be averaged over the cyclotron motion. The new equation is called drift kinetic equation. Furthermore, it is possible to take into account finite Larmor radius effects by adding gyroaveraging and polarization drift into the drift kinetic equation, leading to the gyrokinetic model,[17] which for magnetized plasmas gives an interesting way to study turbulence. This gyrokinetic approximation allows reducing the 3D velocity space into a one-dimensional space ($v_\parallel$) together with the magnetic moment $\mu = m v_\perp^2 / 2B$, which appears as a label. However, solving the resulting equations is still a nontrivial task even in cylindrical geometry.[5,6,18–21]

An alternative approach based on the so-called water-bag model[22] can be considered. This representation of the distribution function is not an approximation but rather a special class of initial conditions allowing one to reduce the full kinetic Vlasov equation into a set of hydrodynamic equations while keeping its kinetic character. In the water-bag model, a discrete distribution function f taking the form of a multisteplike function of the parallel velocity variable is used in place of the continuous distribution function.

Recently, a gyro-water-bag (GWB) model has been developed[22,23] to investigate ion-temperature-gradient modes in a collisionless magnetized plasma. Using a water-bag description for ions imposes collisionless ions. On the other hand, electron-neutral collisions are needed to describe collisional drift waves.

Compared to Refs. 22 and 23, the idea of this paper is to introduce in our ion gyro-water-bag model electron-neutral collisions into the electron response. Ions are always assumed to be collisionless and well described by the Vlasov equation and the water-bag model. This collisional gyro-water-bag model (CGWB) is able to describe both collisional drift waves and ITG instabilities, taking into account the possible interactions between waves and ions. The goal of this work is to investigate the low-frequency instabilities in a laboratory magnetized plasma column using the CGWB model.

The paper is organized as follows. The gyrokinetic model is described in Sec. II and the water bag is introduced in Sec. III. The linear analysis of the new model is presented in Sec. IV. Fluid model, experimental, and CGWB linear results are compared in Sec. V. Kinetic effects on collisional drift waves are studied in Sec. VI. The study of the transition from drift waves to ITG instabilities is presented in Sec. VII. The main results are summarized and conclusions are drawn in Sec. VIII.

II. THE KINETIC MODEL

We consider a cylindrical plasma of radius R. The plasma is confined by a uniform magnetic field $\mathbf{B} = B\mathbf{u}_z$, where $\mathbf{u}_z$ is along the axial direction. The plasma can be weakly or fully ionized. Three species can be considered: the neutral gas, the electron fluid which is free to collide and to exchange momentum with the neutral gas, and finally the ion fluid. Ion-neutral collisions are neglected. It is also assumed that fluctuations of the magnetic field are negligible. The coupling between both ion and electron fluids occurs through the quasineutrality equation $n_e = Z_i n_i$, Z_i being the ionic charge.

A. The ion drift kinetic Vlasov equation

When the ion thermal velocity is close to the phase velocity ($v_{Ti} \lesssim v_\phi$) resonant interactions between waves and particles can play an important role in determining the instability growth rate. Moreover, as ion-neutral collisions are neglected, a more basic kinetic model that directly determines the distribution function is required. The first step is to use a drift kinetic model[18] where trajectories are governed by the guiding-center trajectories, which needs to satisfy $\omega \ll \omega_{Ci}$, where ω is the wave pulsation, and ω_{Ci} is the cyclotron pulsation; i.e., time variations of the plasma are slow as compared to gyration frequency. In cylindrical geometry with $\mathbf{B}$ constant, the only drift to take into account is the electric drift. The ion guiding-center velocity $\mathbf{v}$ is then

$$\mathbf{v} = v_\| \mathbf{u}_z + \frac{\mathbf{E} \times \mathbf{B}}{B^2}, \tag{1}$$

where the electric field $\mathbf{E} = -\nabla \phi$ is due to the perturbation. In this paper the z subscript (or $\|$) denotes the direction parallel to $\mathbf{B}$, and the $\perp$ subscript the direction perpendicular to $\mathbf{B}$. For $\dot{v}_\|$, we get

$$\dot{v}_\| = -\frac{q}{m_i} \nabla_\| \phi. \tag{2}$$

Therefore, the drift-kinetic Vlasov equation can be written as follows:[18,22]

$$\frac{\partial f}{\partial t} - \frac{1}{rB} \frac{\partial \phi}{\partial \theta} \frac{\partial f}{\partial r} + \frac{1}{rB} \frac{\partial \phi}{\partial r} \frac{\partial f}{\partial \theta} - \frac{q}{m_i} \frac{\partial \phi}{\partial z} \frac{\partial f}{\partial v_\|} + v_\| \frac{\partial f}{\partial z} = 0, \tag{3}$$

where f is the ion guiding-center distribution function.

B. The electron response

The approach taken here is to assume that the phase velocity of the instabilities is much lower than the electron thermal velocity. Moreover, electron-neutral collisions are considered. Consequently, we assumed kinetic effects to be negligible so that the electron distribution function is close to a Maxwellian, which enables us to use a fluid model with an isothermal compression to close the system of equations. A viscosity term is introduced into the fluid equation of motion to take into account electron-neutral collisions.

As seen before, perturbations are assumed to be electrostatic. For electrons the following set of equations is used:

- the fluid equation of motion:

$$m_e n_e \left[\frac{\partial \mathbf{v}_e}{\partial t} + (\mathbf{v}_e \cdot \nabla) \mathbf{v}_e \right] = -e n_e (\mathbf{E} + \mathbf{v}_e \times \mathbf{B}) - \nabla p_e$$
$$- m_e n_e \nu_{en} \mathbf{v}_e, \tag{4}$$

where ν_{en} is the electron-neutral collision rate.
- the continuity equation:

$$\frac{\partial n_e}{\partial t} + \nabla \cdot (n_e \mathbf{v}_e) = 0. \tag{5}$$

Assuming an adiabatic electron response in the direction parallel to the magnetic field lines (if collisions are neglected), the linearized density perturbation is

$$n_{e_1} = n_{e_0} \left(\frac{e\phi}{KT_e} \right), \tag{6}$$

where n_{e_0} is the equilibrium density. The perturbation part is indicated by the subscript "1." ϕ is the perturbed potential (there is no potential at equilibrium). This is equivalent to neglecting the electron inertia for the parallel electron motion. We treat only linear, small amplitude fluctuations.

Furthermore, in this paper we need an accurate treatment of the collisional drift waves so that electron-neutral collisions have to be considered. Assuming plane-wave perturbations, we get the following linearized density perturbation:[13]

$$n_{e_1} = n_{e_0} \frac{e\phi}{KT_e} \left[\frac{\omega^* + i\gamma_\parallel}{\omega - \omega_0 + i\gamma_\parallel} \right] \tag{7}$$

with

$$\omega^* = -\frac{KT_e}{eB} k_\theta \partial_r \ln n_{e_0}, \tag{8}$$

$$\gamma_\parallel = \frac{k_\parallel^2 KT_e}{m_e \nu_{en}}, \tag{9}$$

$$\omega_0 = k_\parallel v_{\parallel_0}, \tag{10}$$

where ω^* is the electron diamagnetic frequency, $k_\parallel$ is the parallel wave number, and $v_{\parallel_0}$ is the electron drift velocity in the z direction since in our model a possible electron drift along the magnetic field lines may occur.

C. Gyroaveraging and polarization drift

Finite Larmor radius (FLR) effects are ordinarily taken into account by averaging over the gyromotion of an ion and by introducing the polarization drift. Thus, the ions at a given position, on average, feel a slightly different electric drift velocity than the electrons which are subject to the same electric field. Physically, the term is small but can lead to rather important effects due to charge separation. Therefore, finite Larmor radius corrections are taken into account here by introducing gyroaveraging and polarization drift into the drift kinetic model. Mathematically speaking, the corrections change the order of the equation.

The ion guiding-center density at a position **r** and time t is given by the integral of the ion guiding-center distribution function. In order to determine the effective ion density, we have to replace every guiding-center by a circular charge distribution.[24]

The operation going from a given guiding-center density of particles to its corresponding particle density is equivalent to a filter operation and is obtained through an integral operator that takes into account the FLR correction. This operator is represented by the Bessel function J_0 in wavenumber space. When averaging the Larmor radius over a Maxwellian the function J_0 can be approximated by an exponential function of the thermal velocity and the cyclotron frequency.[24] Therefore, it is possible to determine the effective electric field.

Note that electrons are assumed to move with a zero Larmor radius so that the electron density coincides with the guiding-center density (the Larmor radius is much smaller for electrons than for ions).

It must be pointed out that the FLR gyroaverage operator has to be applied both to the ion density in the quasineutrality equation, and to the effective potential before its introduction into the drift kinetic Vlasov equation (3).

The electric field induced by the plasma instabilities is varying in time. The polarization drift is a second-order term in ω/ω_{Ci} (if it is assumed that the characteristic time of variation of the electric field is large compared to a gyroperiod). The Larmor radius changes when the charged particle

orbits its guiding-center, leading to a drift perpendicular to the magnetic field, and is called polarization drift, which can be written

$$\mathbf{v}_P = \frac{1}{\omega_{Ci}B} \frac{d\mathbf{E}}{dt}. \tag{11}$$

The polarization drift can be explicitly introduced in the Vlasov equation or can be written as a perturbed ion density so that the quasineutrality equation reads[18]

$$n_e = Z_i \left[n_i + \nabla_\perp \cdot \left(\frac{n_i}{\omega_{Ci}B} \nabla_\perp \phi \right) \right]. \tag{12}$$

The second term on the right hand side corresponds to the linearized polarization term.

Finally, the ion Vlasov equation takes the following form:

$$\frac{\partial f}{\partial t} - \frac{1}{rB} \frac{\partial \langle \phi \rangle}{\partial \theta} \frac{\partial f}{\partial r} + \frac{1}{rB} \frac{\partial \langle \phi \rangle}{\partial r} \frac{\partial f}{\partial \theta} - \frac{q}{m_i} \frac{\partial \langle \phi \rangle}{\partial z} \frac{\partial f}{\partial v_\parallel} + v_\parallel \frac{\partial f}{\partial z} = 0, \tag{13}$$

and the quasineutrality equation can be rewritten in the following way:

$$n_e = Z_i \left[\langle n_i \rangle + \nabla_\perp \cdot \left(\frac{n_i}{\omega_{Ci}B} \nabla_\perp \phi \right) \right], \tag{14}$$

where $\langle \cdot \rangle$ represents the gyroaveraged operator that takes into account the finite Larmor radius correction. Note that for the right hand side term of Eq. (14) (polarization drift) n_i and ϕ are not gyroaveraged because the polarization drift already corresponds to a correction.

III. INTRODUCING THE WATER-BAG MODEL

Since the ion distribution function $f(\mathbf{r}, v_\parallel)$ (where $\mathbf{r} = r, \theta, z$) takes into account only one velocity component (namely, $v_\parallel$ parallel to **B**) it is valuable to turn to a water-bag solution (see Refs. 21 and 22).

To sketch out the water-bag modeling and moreover the differences with a usual kinetic description, let us consider a special initial condition in which the distribution function f takes on a constant value A between two contours $v^+(\mathbf{r})$ and $v^-(\mathbf{r})$ in the $(\mathbf{r}, v_\parallel)$ phase space, and zero outside. According to Liouville's phase space conservation property f remains constant in time between the contours and of course zero outside.

Therefore, the problem is entirely described by the knowledge of two functions $v^+(\mathbf{r}, t)$ and $v^-(\mathbf{r}, t)$, which are the contours of the phase space fluid called "water bag." The generalization to the "multiple water bag" is straightforward. Let us consider $2N$ contours in phase space $v_j^+(\mathbf{r})$ and $v_j^-(\mathbf{r})$, where $j = 1, \ldots, N$. We get a N-bag system where the distribution function takes on N different constant values F_j (see Figs. 1 and 2). The time evolution of the system is completely described by the knowledge of the contours. We obtain a set of hydrodynamic equations, where the system behaves as N fluids coupled together by the electromagnetic fields (in our case, the quasineutrality).
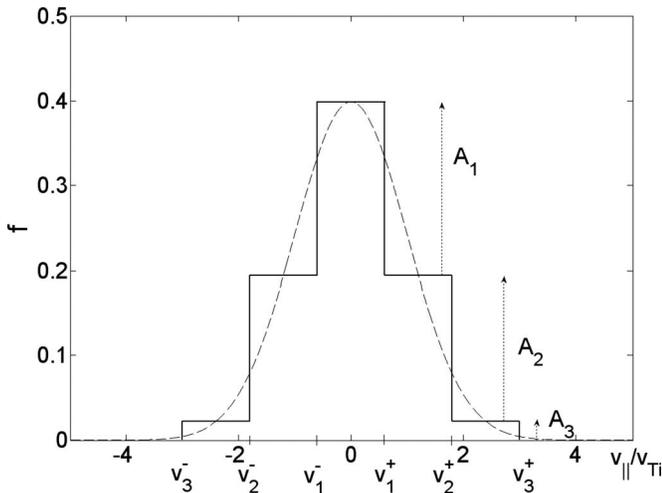
FIG. 1. The multi-water-bag distribution function plotted against parallel velocity, for $N=3$ bags with $v_{max}=3v_{T_i}$. The jth bag is a rectangle with a height A_j and a length $(v_j^+ - v_j^-)$. The height of the steps remains constant, while parallel velocity is time dependent.

Introducing the bag heights $A_j = F_j - F_{j+1}$ as shown in Fig. 1 the distribution function reads

$$f(\mathbf{r}, v_\parallel, t) = \sum_{j=1}^{N} A_j [H(v_\parallel - v_j^-) - H(v_\parallel - v_j^+)], \qquad (15)$$

where H is the Heaviside unit step function. The relative ion density of the jth bag is defined by $\alpha_j = A_j (v_j^+ - v_j^-)/n_0$, where n_0 is the plasma density at equilibrium.

In Eq. (15), j is nothing but a label since no differential operation is carried out on the variable $v_\parallel$. What we actually do is to bunch together particles within the same bag j and let each bag evolve. Of course, the different bags are coupled through the quasineutrality equation.

This operation appears as an *exact* reduction of the phase space dimension (elimination of the velocity variable $v_\parallel$) in the sense that the water-bag concept makes full use of the Liouville invariance in phase space: the fact that the A_j's are
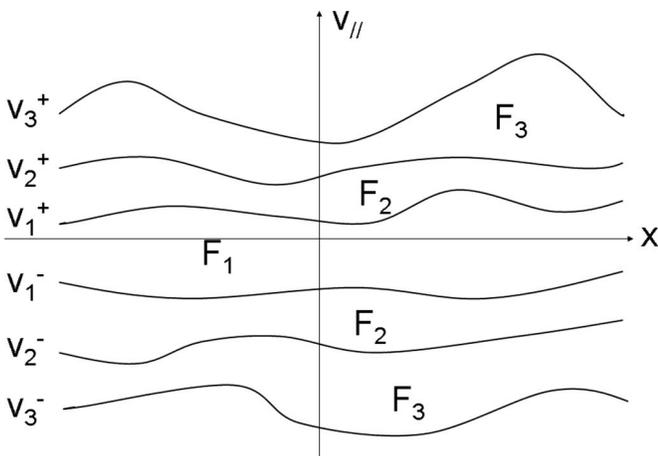
FIG. 2. Bag contours in the phase space $(x, v_\parallel)$ for a three-bag system. Between two contours, the distribution function f remains equal to a constant F_j. The properties of the system are completely described by the knowledge of the contours.

constant in time is nothing but a straightforward consequence of the Vlasov conservation $Df/Dt=0$. Of course, the eliminated velocity reappears in the various bags j, and if a precise description of a continuous distribution is needed, a larger N is required. On the other hand, there is no mathematical lower bound on N and from a physical point of view many interesting results can even be obtained with N as small as 1 for electrostatic plasma. For magnetized plasma, $N=2$ or 3 allow more analytical approaches.[22]

On the contrary, in the usual gyrokinetic description, the exchange of velocity is described by a differential operator. From a numerical point of view, this operator has to be approximated by some finite difference scheme. Consequently, a minimum size for the mesh in the velocity space is required and we are faced with the usual sampling problem. If it can be claimed that the $v_\parallel$-gradients of the distribution function remain weak enough for some class of problems, then a rough sampling might be acceptable. However, it is well known in kinetic theory that wave-particle interaction is often not so obvious. For instance, steep gradients in the velocity space can be the signature of strong wave-particle interaction and there is the need for a higher numerical resolution of any Vlasov code, while a water-bag description can still be used with a small bag number.

Thus, the water bag offers an exact description of the plasma dynamics even with a small bag number, allowing more analytical studies and bringing the link between the hydrodynamic description and the full Vlasov one. Of course, a special initial preparation of the plasma is required (namely, a Lebesgue subdivision as compared to the Riemann subdivision used in any numerical sampling). Furthermore, there is no constraint on the shape of the distribution function which can be very far from a Maxwellian. Once initial data have been prepared using Lebesgue subdivision, the gyro-water-bag equations give the exact weak (in the sense of the theory of distribution) solution of the Vlasov equation corresponding to this initial data. Any initial condition (continuous or not) which is integrable with respect to the Lebesgue measure can be approximated accurately with larger N. Therefore, if we need a precise description of a continuous distribution, it is clear that a larger N is needed; but even if the numerical effort is close to a standard discretization of the velocity space in a regular Vlasov code (using $2N+1$ mesh points), the use of an exact water-bag sampling should give better results than approximating the corresponding differential operator. As a matter of fact, a small bag number (not more than 10) has been shown to be sufficient to correctly describe the ion-temperature-gradient (ITG) instability observed in fusion plasmas (see Ref. 22).

To turn back more precisely to our gyrokinetic model described in Sec. II above, and using the ion water-bag distribution function (15), we obtain the contour equations

$$\partial_t v_j^\pm + \mathbf{v}_E \cdot \nabla_\perp v_j^\pm + v_j^\pm \partial_z v_j^\pm = \frac{q_i E_\parallel}{m_i}, \qquad (16)$$

where $\mathbf{v}_E$ is the electric drift. The idea behind the CGWB model is to connect this ion water-bag description with the electron-neutral collisional model involved in the electron

response equation (7). Equations (16) together with Eqs. (7) and (14) form the basis of the CGWB model, where $n_i = \Sigma A_j(v_j^+ - v_j^-)$ couples the different bags.

The full numerical implementation of the water bag for gyrokinetic purpose (the so-called gyro-water-bag model) is discussed in detail in Ref. 23. More precisely with the aim of determining the initial water-bag parameters (the A_j's), it is shown how to consider the equivalence of the multiple water bag with the corresponding continuous distribution function in the fluid momentum sense (providing momenta of order up to $2(N-1)$ are taken into account).

IV. LINEAR STUDY OF THE COLLISIONAL-GYRO-WATER-BAG MODEL

A direct illustration of the ability of the collisional-gyro-water-bag (CGWB) model to reproduce the physical features of the drift waves and ITG instabilities is given by the linear analysis of Eqs. (7) and (13) and the quasineutrality equation (14). Velocities and the plasma potential are separated from their perturbations, keeping only the first-order perturbations. a_j are the contour velocities at equilibrium ($v_j^{\pm} = \pm a_j + \delta v_j^{\pm}$), f is an even function of v at equilibrium. There is no electric field at equilibrium. Considering a plasma slab geometry, these perturbations are projected on a Fourier basis in θ and z directions:

$$\delta v_j^{\pm} = \delta v_{j_{m\omega}}^{\pm}(r)\exp[i(m\theta + k_{\parallel}z - \omega t)] \tag{17}$$

and

$$\phi = \phi_{m\omega}(r)\exp[i(m\theta + k_{\parallel}z - \omega t)]. \tag{18}$$

Note that the $\exp(-i\omega t)$ dependence implies an unstable perturbation if $\mathrm{Im}(\omega) > 0$. According to these assumptions and using Eqs. (7), (14), and (16), the linearized dispersion relation can be written

$$\frac{\omega^* + i\gamma_{\parallel}}{\omega - \omega_0 + i\gamma_{\parallel}} + \delta - J_0^2\sum_{j=1}^{N}\alpha_j\frac{Z_i\omega_{cs}^2 + \omega_j^*\omega}{\omega^2 - k_{\parallel}^2 a_j^2} = 0 = \varepsilon(\omega), \tag{19}$$

where

$$\delta = Z_i\rho_s^2(\kappa(r) + k_{\theta}^2) \tag{20}$$

or

$$\delta = Z_i^* r_{L_i}^2(\kappa(r) + k_{\theta}^2) \tag{21}$$

and $\omega_{cs}^2 = k_{\parallel}^2 c_s^2$, J_0 is the gyroaverage operator, $Z_i^* = Z_i/\tau$ with $\tau = T_i/T_e$, $\omega_j^* = -KT_e/eBk_{\theta}\partial_r\ln a_j$, $c_s = \sqrt{KT_e/m_i}$, $\rho_s = c_s/\omega_{Ci}$, $k_{\theta} = m/r$, m is the azimuthal mode, and

$$\kappa(r) = -\left[\frac{\partial^2 g}{\partial r^2} + \left(\frac{\partial g}{\partial r}\right)^2 + \left(\frac{\partial\ln n_0}{\partial r} + \frac{1}{r}\right)\frac{\partial g}{\partial r}\right], \tag{22}$$

where $g(r)$ depends on the radial profile of the potential amplitude:

$$\phi_{m\omega}(r) = \phi_{0_{m\omega}}\exp[g(r)]. \tag{23}$$

In a linear device, the ratio of the observed frequency to the ion cyclotron frequency is much greater than for a tokamak, even if this ratio is always much less than 1. Therefore,

the effect of the polarization drift is very important, altering the results obtained when gyroaverage and polarization drift are not taken into account.

In the one-bag case, a nearly fluid model[22] is obtained, which should give close results. For this one-bag case, the dispersion relation (19) is

$$i\frac{\delta}{\gamma_{\parallel}}\omega^3 - \left[1 + \delta + i\frac{\omega_0\delta + \omega^*(J_0^2 - 1)}{\gamma_{\parallel}}\right]\omega^2$$
$$+ \left[J_0^2\omega^* + i\frac{J_0^2(\omega_0\omega^* - Z_i\omega_{cs}^2) - \omega_{\parallel}^2\delta}{\gamma_{\parallel}}\right]\omega + \omega_{\parallel}^2(1 + \delta)$$
$$+ J_0^2 Z_i\omega_{cs}^2 + i\left[\frac{J_0^2 Z_i\omega_{cs}^2\omega_0 + (\omega_0\delta - \omega^*)\omega_{\parallel}^2}{\gamma_{\parallel}}\right]$$
$$= 0 = \varepsilon(\omega), \tag{24}$$

where $\omega_{\parallel} = \sqrt{3}k_{\parallel}v_{Ti}$ and $v_{Ti} = \sqrt{KT_i/m_i}$.

The gyroaveraged and polarization terms (finite Larmor radius corrections) introduced into the equations can play a more or less important role in describing the instabilities. Indeed, if $k_{\theta}r_{L_i}$ is small compared to 1, the gyroaverage operator can be expressed in the k-space:[24]

$$J_0 \sim 1 - \frac{\varepsilon_{\mathrm{gyr}}^2}{2}, \tag{25}$$

where $\varepsilon_{\mathrm{gyr}} = k_{\theta}r_{L_i}$, and r_{L_i} is the averaged Larmor radius assuming a Maxwellian distribution for the perpendicular velocity. Moreover, the polarization term is of order $\varepsilon_{\mathrm{pol}}^2$ with [assuming that $\kappa(r)$ is as the same order as k_{θ}^2]

$$\varepsilon_{\mathrm{pol}} = \sqrt{Z_i}\rho_s k_{\theta}. \tag{26}$$

Gyroaverage and polarization drift are corrections, respectively, of order $\varepsilon_{\mathrm{gyr}}^2$ and $\varepsilon_{\mathrm{pol}}^2$. The ratio ($\varepsilon^2 = \varepsilon_{\mathrm{gyr}}^2/\varepsilon_{\mathrm{pol}}^2$) is equal to

$$\varepsilon^2 = \frac{\tau}{Z_i}. \tag{27}$$

In a tokamak plasma, τ is approximately equal to 1. In that case, gyroaverage and polarization drift corrections are of the same order, according to the gyro-ordering for tokamaks.

In a laboratory plasma device, the τ factor can be as small as $1/50$, for example. The correction due to the polarization drift is therefore 50 times greater than that of gyroaveraging.

V. COMPARISON WITH A FLUID MODEL AND EXPERIMENTAL RESULTS

The CGWB is thus able to describe the collisional drift waves and the ITG instabilities. In this section the validation of the model is performed by comparing our new CGWB model, a fluid model and experimental results.

A. Collisional drift waves

We first look at the collisional drift waves case. This class of instabilities involves waves which may become unstable under the presence of a density gradient, electron-neutral collisions, and a parallel electron drift.

TABLE I. Collisional drift waves growth rate for a variety of plasma conditions. The $m=2$ mode is dominant.

Mode	1	2	3	4
r_0 (10^{-2} m)	1.21	1.54	1.65	1.66
κ_n (m^{-1})	−87	−112	−120	−120
Δr (10^{-2} m)	0.8	0.6	0.5	0.45
Growth rate (10^4 s^{-1})	1.04	1.3	1.27	1.21

Our CGWB model can be used only if ion-neutral collisions can be neglected since the CGWB model requires phase space conservation of the Vlasov equation ($df/dt=0$) for ions, as seen in Sec. III. On the other hand, electron-neutral collisions are required for collisional drift waves to occur. Therefore, we have to carefully look at the problem of ion-neutral collisions. To do that, the linear instability growth rate γ given in Ref. 13 in the case of a slab fluid model will be studied:

$$\gamma = \gamma_+ - \gamma_-, \quad (28)$$

where

$$\gamma_+ = \frac{b}{1+b}\left(\frac{\omega^{*2}}{\gamma_\parallel (1+b)^2} + \frac{\omega_0 \omega^*}{b\gamma_\parallel}\right) \quad (29)$$

and

$$\gamma_- = \frac{b}{1+b}\nu_i \quad (30)$$

and where $b = k_\theta^2 \rho_s^2$.

It is clear that electron-neutral collisions are destabilizing while ion-neutral collisions are stabilizing. Thus, neglecting ion-neutral collisions is equivalent to neglecting their stabilizing effect.

First a comparison between results obtained by both CGWB and nonlocal fluid model given in Ref. 13 is provided. An argon plasma is considered. Only one bag is chosen for the CGWB model, so that the resulting set of equations is equivalent to the fluid model. The function $g(r)$ is

$$g(r) = -\frac{(r-r_0)^2}{(\Delta r)^2}, \quad (31)$$

where r_0 and Δr are chosen to fit the perturbation functions $\phi_{m\omega}(r)$ obtained in Ref. 13 for azimuthal modes going from $m=1$ to $m=4$. The other parameters are the same as Ref. 13; namely, $T_e=2$ eV, $B=0.2$ T, $\nu_{en}=2.6\times10^6$ s^{-1}, $v_{\parallel_0}=0.2v_{Te}$, and $\lambda_z=3$ m. The density profile is assumed to be Gaussian, i.e., $n_0=n_{0_{max}}\exp(-r^2/r_n^2)$, with $r_n=1.66$ cm. The results are given for $r=r_0$, where the perturbation is expected to be maximum. Note that the knowledge of r_0 and Δr is necessary to calculate $\kappa(r)$ [Eq. (22)] even if $g(r_0)=0$. Moreover, $\kappa_n(r=r_0)=-(2r/r_n^2)_{r=r_0}$, where $\kappa_n=\partial_r \ln n_0$. The parameters r_0, Δr, and κ_n are summarized in Table I.

The main difference between CGWB and fluid models relates to ion-neutral collisions, which are neglected in CGWB. Indeed, the large magnitude of the magnetic field allows us to neglect ion-neutral collisions: the ratio γ_+/γ_- is
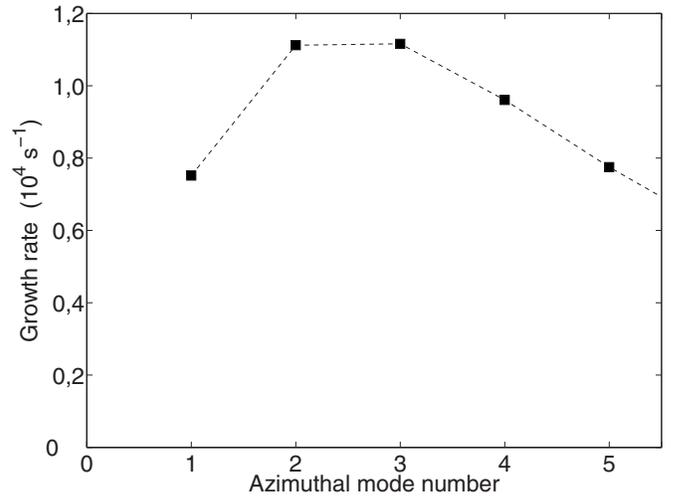
FIG. 3. Instability growth rate vs azimuthal mode number for collisional drift waves, with parameters from Ref. 13.

greater than 40 for $m=1$ and greater than 10 for $m=5$. Moreover, ω/ω_{C_i} is less than 0.1, which allows us to use the gyrokinetic model.

The CGWB results are shown Table I and Fig. 3. The linear growth rate of the instability is plotted against the azimuthal mode m. A maximum growth rate is equal to $\gamma=1.3\times10^4$ s^{-1} in the case $m=2$. These results obtained by the CGWB model are in full agreement with the values predicted by the nonlocal cylindrical fluid model.[13]

The next step is now to validate the CGWB model by comparing the linear analytical investigation of collisional drift waves and the experimental results obtained from the laboratory magnetized plasma column Mirabelle.[7,25–28] The main plasma parameters are given in Ref. 27.

In a linear column like the Mirabelle device, collisional drift waves are due to electron-neutral collisions, an electron drift along the magnetic field lines, and a density gradient. The estimated uniform ion temperature is approximately equal to 0.03 eV (no temperature gradient). Actually, the value of $T_i=0.03$ eV was found by laser-diagnostic measurements performed in a thermionic discharge.[29,30] A measurement setup[27,28] allows us to obtain density, temperature, potential profiles, and the parallel wave number.

The plasma diameter can be restricted by inserting a limiter at the entrance of the column. The diameter of the plasma column is smaller than the diameter of the containing tube. In this case instabilities are drift waves as long as the magnetic field is strong enough so that the limiter does not play any role in confining the plasma. In this situation with a flat potential profile, instabilities are identified as being drift waves instabilities.[27] Our different assumptions are satisfied due to a strong magnetic field: ω/ω_{C_i} is approximately 0.1 for $B=0.1$ T (always less than 0.2 for this magnetic field).

The data of Mirabelle experiments carried out previously[27,28] are used. The function $g(r)$ [Eq. (31)] is the same as used before. The parameters $r_0=4$ cm, $r=r_0$, and $\Delta r=2.5$ cm are chosen so as to fit the radial experimental profile of the amplitude of the perturbations. The other parameters are: $B=0.1$ T, $T_e=2$ eV, $\nu_{en}=1.3\times10^6$ s^{-1} (in

Mirabelle the pressure is at least twice lower than that of in Ref. 13, so that an electron-neutral collision rate divided by 2 is considered here), $k_\parallel = 2$ m^{-1}, and $\kappa_n = -30$ m^{-1}, where $\kappa_n = \partial_r \ln n_0$. For an argon plasma, $m_i = 6.6 \times 10^{-26}$ kg. For $B = 0.1$ T, the assumption $\gamma_+ / \gamma_- \gg 1$ is satisfied only for $m < 5$ ($\gamma_+ / \gamma_- > 5$ for $v_{\parallel 0} = 0.2 v_{Te}$, and $\gamma_+ / \gamma_- > 40$ for $v_{\parallel 0} = 2 v_{Te}$, with $\nu_{in} = 0.5 \times 10^6$ s^{-1}). During the experiments reported here, a coherent mode $m=2$ or $m=1$ is recorded,[27] whereas for lower magnitudes of the magnetic field (for example, $B = 0.04$ T), higher modes until $m=7$ can be obtained.[25] Thus, only results for a high magnetic field ($B = 0.1$ T) for which only low modes occur are presented in this paper, with the aim of making sure that the assumptions of the CGWB model are satisfied.

In Mirabelle experiments, the bias of an insulated internal metallic tube is one of the dynamical control parameters of the experimental setup.[25] The azimuthal mode number decreases with the increase of biasing in the tube; meanwhile, the frequency increases. Next the mode suddenly changes for a lower mode with a lower frequency.

The goal is to retrieve this behavior from the CGWB model, the increase of the bias leading to an increase of the axial electronic drift ($v_{\parallel 0}$). At the same time we have experimentally observed that the background density profiles are not altered. Consequently, we only consider the increase of the parallel electron drift in our simulation.

Without gyroaveraging and any polarization drift, i.e., without any FLR effect, the CGWB model predicts an increasing growth rate with m for m modes going from 1 to 5, for which the stabilizing effect of γ_- [Eq. (28)] and the ion viscosity can be neglected. This result disagrees with experimental results. When gyroaveraging is applied, the CGWB model keeps predicting an increasing growth rate with m. Polarization drift has to be taken into account to predict a decrease of the growth rate with increasing m and to be in a good agreement with the fluid model and experimental results. In a device like Mirabelle, the polarization drift is much higher than the gyroaverage. Indeed τ is roughly equal to 0.01, so according to Eq. (27) the polarization term is approximately 50 to 100 times greater than the gyroaverage term.

Therefore, Eq. (24) with only one bag exhibits results shown in Figs. 4 and 5. In Fig. 4 it can be seen that the transition from $m=2$ to $m=1$ is well described for $v_{\parallel 0}$ going from $2 v_{Te}$ to $10 v_{Te}$. Moreover, the frequencies in the range 5–10 kHz given by the CGWB model are in good agreement with the frequencies recorded in the device. The instability linear growth rates are depicted in Fig. 5, which shows the dependence of $\gamma = \text{Im}(\omega)$ on m, for two values of the electron parallel drift. A transition from the most unstable mode $m=2$ for $v_{\parallel 0} = 4 v_{Te}$ to the $m=1$ mode for $v_{\parallel 0} = 8 v_{Te}$ is predicted. This behavior is in a very good agreement with the experimental result; i.e., m decreases with an increasing electron parallel drift.

For such parameters, the similarity between one and several bags must be pointed out. Actually, the instability phase velocity is much greater than the ion thermal velocity. The plasma-wave interactions have very low influence on the collisional drift waves dynamics in this case. It must be noted
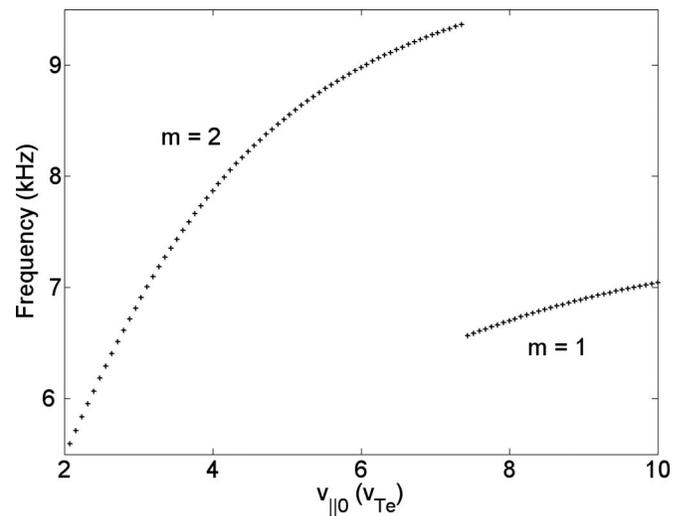
FIG. 4. Frequency of the most unstable mode plotted against the parallel electron drift $v_{\parallel 0}$, with FLR effects, and with one bag ($N=1$).

that for the CGWB model, in the case of one bag the temperature profile is related to the density profile.[22] This link is broken if $N > 1$. Thus, in this one-bag case an ion temperature profile is imposed by the CGWB model, while it does not exist in Mirabelle. However, this ion temperature profile does not influence the results (it does not trigger an ITG mode), which would be the same if two or more bags were chosen with a flat temperature profile.

Also note that in this paper the CGWB model is linearized so that nonlinear phenomena cannot be taken into account. Only a numerical solution of the nonlinear equations will make it possible to include these effects and avoid the slab assumption.
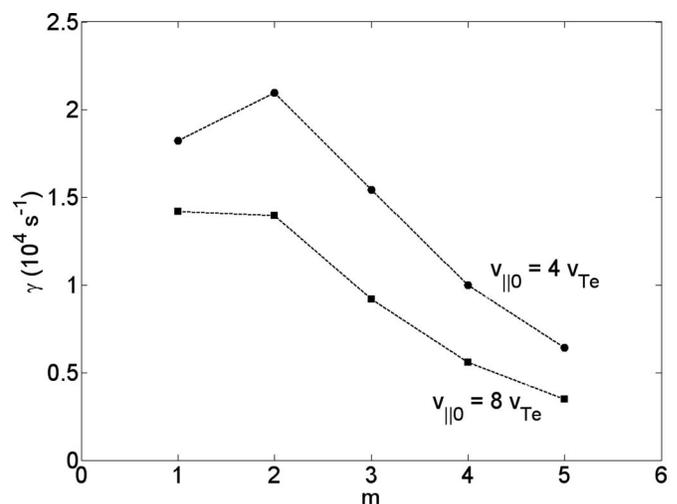
FIG. 5. Instability growth rate vs azimuthal mode number. One curve pertains to $v_{\parallel 0} = 4 v_{Te}$ ($m=2$ is predicted to exhibit the maximum growth rate) and the other one pertains to $v_{\parallel 0} = 8 v_{Te}$ ($m=1$ is predicted to exhibit the maximum growth rate).

B. Ion-temperature-gradient instability

The next paragraph is devoted to the ability of CGWB model to describe ITG instabilities for which an ion temperature gradient is needed.

The parameter $\eta = \kappa_T / \kappa_n = \partial_r \ln T_i / \partial_r \ln n_0$ (Refs. [31] and [32]) has to exceed a critical value to observe an ITG instability. This parameter can be increased either by flattening the density gradient or by increasing the ion temperature gradient.

We focus here on the Columbia Linear Machine (CLM).[33] CLM is a linear device with radiofrequency heating employed to heat the core of the plasma column and to produce a peaked ion temperature profile. Furthermore, the mesh for ion heating reduces the density in the central core and helps to reduce the density gradient. Therefore, this heating can produce high values of η.

The goal is to compare the CLM experimental results[12] with our theoretical CGWB model of the ITG instability, previously used for fusion plasmas.[22,23] A hydrogen plasma is produced in CLM. The magnetic field is $B = 0.1$ T. For such a magnetic field, the assumption of collisionless ions is well satisfied, and $\omega / \omega_{C_i} < 0.01$. An ion parallel drift exists. However, this drift is slow compared to the ion thermal velocity.[12] Thus, a water-bag distribution function can be chosen for ions with a zero mean velocity.

Typical plasma parameters in the experimental region of the device are:[12] $\tau = 3$, $T_i = 14$ eV, $B = 0.1$ T, and $r = 1.75$ cm (where the temperature gradient is maximum). Equation (19) is solved with $N = 20$ bags. Only H_2^+ ions are considered, so $Z_i = 1$ and $m_i = 3.32 \times 10^{-27}$ kg. The $g(r)$ function (31), with r_0 and Δr is chosen to fit the observed experimental profile of the amplitude of the perturbations. Data given in Ref. [12] are used: $r = r_0$ and 0.5 cm $\leq \Delta r \leq 1$ cm. In addition, -131 m$^{-1} \leq \kappa_T \leq -91$ m^{-1}, -33 m$^{-1} \leq \kappa_n \leq -3$ m^{-1}, and $2\pi/6$ m$^{-1} \leq k_\parallel \leq 2\pi/3$ m^{-1}, where $\kappa_T = \partial_r \ln T_i$ and $\kappa_n = \partial_r \ln n_0$.

For these parameters, the destabilizing terms are temperature and density gradients. The collision rates can be neglected. CGWB results are shown Fig. 6. The real frequency is plotted against $k_\parallel$ and κ_n. Error bars on the other parameters κ_T and Δr do not change the obtained frequency range and are not considered. κ_T and Δr are taken to be, respectively, equal to -111 m^{-1} and 0.75 cm. The $m = 2$ mode is always the most unstable mode and the real frequency is negative, meaning that the perturbation propagates in the ion diamagnetic drift direction.

The CGWB results shows that the $m = 2$ mode is always dominant for such parameters, with a real frequency in the range $2 - 11$ kHz. Furthermore, the perturbation propagates in the ion diamagnetic direction, as expected for ITG instabilities.

This ITG mode is confirmed in the CLM device, where a $m = 2$ mode is obtained with a finite parallel wavelength and an azimuthal propagation in the ion diamagnetic drift direction. The real frequency of the mode lies in the $6 - 10$ kHz range, which is in fairly good agreement with CGWB predictions. However, these experimental values are slightly greater than the frequencies given by CGWB, but if error
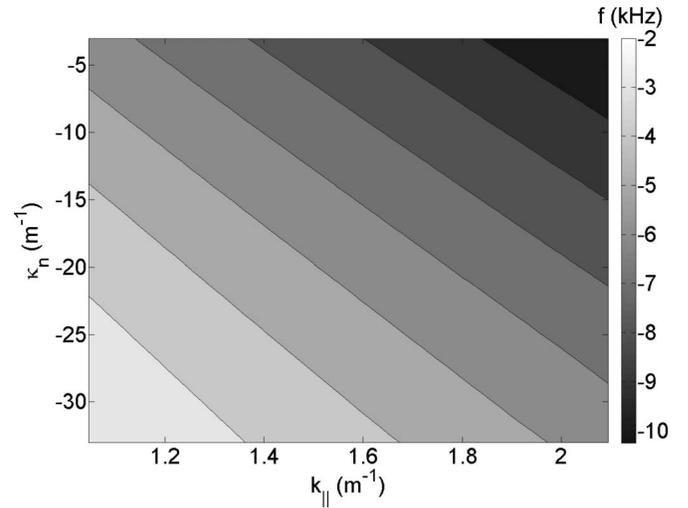
FIG. 6. Instability frequencies obtained by the CGWB model plotted against $k_\parallel$ and κ_n. The real frequencies are in the range $2 - 11$ kHz and instability propagates in the ion diamagnetic direction (ITG instability).

bars and a possible mixing between H^+ and H_2^+ ions are considered, we can conclude that the experimental real frequency of the mode is very close to what is expected from the CGWB dispersion relation.

Also note that for this CLM experiment it is clear from Eq. (27) that polarization drift and gyroaverage are quite equivalent, τ being approximately equal to 3.

VI. ION TEMPERATURE INFLUENCE ON COLLISIONAL DRIFT WAVES

We have previously compared the CGWB model with experimental results. The goal in this part is to study the role of kinetic effects in CGWB on collisional drift waves.

With several bags, the model makes it possible to explore the kinetic aspects of drift waves. In the Mirabelle device, ions being cold the ionic thermal speed is much less than the phase velocity, which points to very weak kinetic phenomena in such a plasma.

Thus, for collisional drift waves kinetic effects will appear only with an increase of the ion temperature, ion thermal velocity being close to phase velocity.

Here we only consider an increase of the ion temperature (without any temperature gradient), and consequently its kinetic effects on the collisional drift waves.

We work within the framework of a Mirabelle-like experiment, in which we would have implemented an ion heating device, as in the Columbia machine, in order to increase the ion temperature and to decrease the κ_n parameter. Here, $\kappa_T = 0$ is assumed in order to avoid ITG instability and to study only kinetic effects on drift waves. We consider again the plasma parameters given in Sec. V: $r_0 = 4$ cm, $r = r_0$, $\Delta r = 2.5$ cm, $T_e = 2$ eV, $\nu_{en} = 1.3 \times 10^6$ s^{-1}, $k_\parallel = 2$ m^{-1}, $\kappa_n = -10$ m^{-1}, and $B = 0.1$ T. The plasma is an argon plasma. We take $T_i = 2$ eV, and $v_{\parallel 0} = v_{Te}$. With this set of parameters, the most unstable mode is $m = 2$.
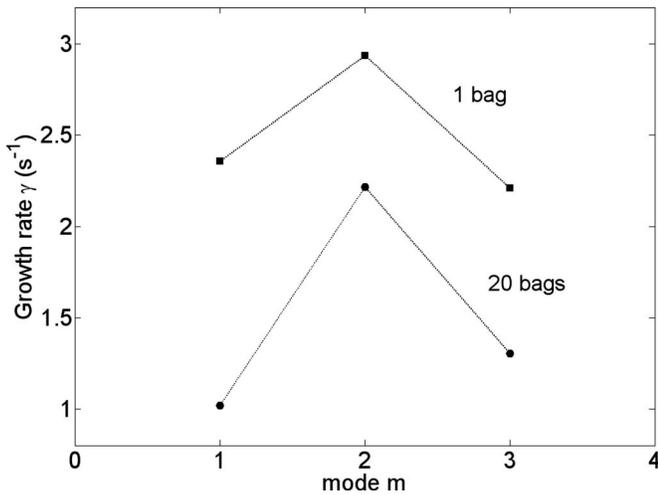
FIG. 7. Instability growth rate plotted against the mode m, in the one-bag case (equivalent to a fluid model), and in the 20-bag case (equivalent to a kinetic model), with $v_{\parallel 0}=v_{Te}$ and $T_i=2$ eV.

FIG. 8. Transition from collisional drift waves to ITG instability. The growth rate of the most unstable mode is plotted against the parameter $\kappa_T = \partial_r \ln T_i$. Drift waves (left side) or ITG instabilities (right side) can be observed as a function of κ_T. If κ_T exceeds a critical value, the ITG instability growth rate becomes rapidly greater than that of drift waves.

Furthermore, let us recall that we have to neglect γ_- as compared to γ_+ for allowing the use of the Vlasov equation for ions. Assuming that the ion-neutral collision rate ν_{in} is proportional to $\sqrt{T_i}$ (since it is proportional to v_{Ti}), we then get $\gamma_+/\gamma_-=6$ with $m=2$. We make the assumption that this ratio is large enough. Note that this ratio becomes larger with increasing $v_{\parallel 0}$ or if a hydrogen plasma is considered instead an argon plasma.

Results are shown in Fig. 7. The instability growth rate is plotted against the mode number m, with $T_i=2$ eV, which corresponds to a thermal velocity equal to 2.2×10^3 m s^{-1}, while the drift wave phase velocity is almost equal to $v_\varphi =5.1\times 10^3$ m s^{-1}, which means $v_{Ti}/v_\varphi=0.43$. Thus, wave-particle interaction effects can be expected. Two curves are presented. The first one with only one bag is equivalent to a fluid one, and indeed is not able to take into account the kinetic effects. In the second one the bag number is large enough ($N=20$, $v_{\max}=5v_{T_i}$) to be equivalent to a continuous kinetic model.

It must be noticed that the instability growth rate clearly decreases with an increasing bag number. This result confirms that the kinetic phenomena play a stabilizing role when the thermal velocity is close to the phase velocity. These observations are in good agreement with the following result: The fluid models overestimate the transport coefficients as compared to those given by the kinetic models. Indeed, using the mixing length estimate and a random walk estimate (a first naive approach) yields a diffusion coefficient proportional to $\gamma_{\max}$, where $\gamma_{\max}$ is the maximum linear growth rate.[2] In the case studied here, the $m=2$ mode remains the most unstable mode while N increases, but with other plasma parameters a different most unstable mode could be observed. Thus, when the ion thermal velocity is comparable to the phase velocity, a kinetic model clearly appears to be the most suitable tool to study these instabilities.
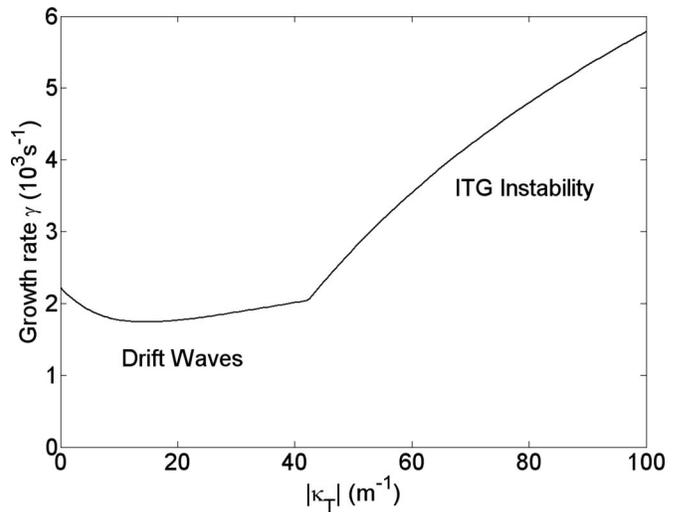
VII. TRANSITION FROM DRIFT WAVES TO ION-TEMPERATURE-GRADIENT (ITG) INSTABILITY

Our model is able to describe simultaneously collisional drift waves and ITG instabilities. For both types of instability the kinetic effects are taken into account.

The goal here is to study the transition from collisional drift waves to ITG instabilities when the parameter $\kappa_T = \partial_r \ln T_i$ increases. If this parameter is zero, only drift waves occur. When κ_T exceeds a critical value, ITG modes become unstable.

The plasma parameters given in the previous section are used: $r_0=4$ cm, $r=r_0$, $\Delta r=2.5$ cm, $T_e=2$ eV, $\nu_{en}=1.3 \times 10^6$ s^{-1}, $k_\parallel=2$ m^{-1}, $\kappa_n=-10$ m^{-1}, and $B=0.1$ T, for an argon plasma. $T_i=2$ eV is chosen and κ_T is in the range $0-10\kappa_n$, with $N=20$ bags up to $5v_{Ti}$. Here, $v_{\parallel 0}=v_{Te}$ is assumed. For this set of parameters, $m=2$ is the most unstable mode.

Results are shown in Fig. 8. For $|\kappa_T|$ in the range $0-42$ m^{-1}, the linear growth rate is about 10^3 s^{-1} and corresponds to collisional drift waves. ITG instability occurs if $|\kappa_T|$ exceeds the critical value $|\kappa_T|=42$ m^{-1}, for which the ITG growth rate is greater than that of drift waves. The linear growth rate keeps increasing with $|\kappa_T|$. Note that the ratio $\eta=\kappa_T/\kappa_n$ is 3.2 at the ITG instability threshold, given by the collisionless GWB model without any parallel drift.[22]

The real pulsation corresponding to this most unstable mode is plotted against the parameter $|\kappa_T|$ (Fig. 9). It can be pointed out that for $|\kappa_T|<42$ m^{-1}, ω_r is greater than zero and is almost equal to the electron diamagnetic pulsation ω^*. Moreover, the perturbation propagates in the electron diamagnetic drift direction as expected for drift waves. Note that $\omega/\omega_{C_i}<0.06$. Moreover, note that the frequency of the drift waves varies with increasing $|\kappa_T|$ because the equation of dispersion (19) depends on ω_j^*, ω_j^* being a function of κ_T.[22]
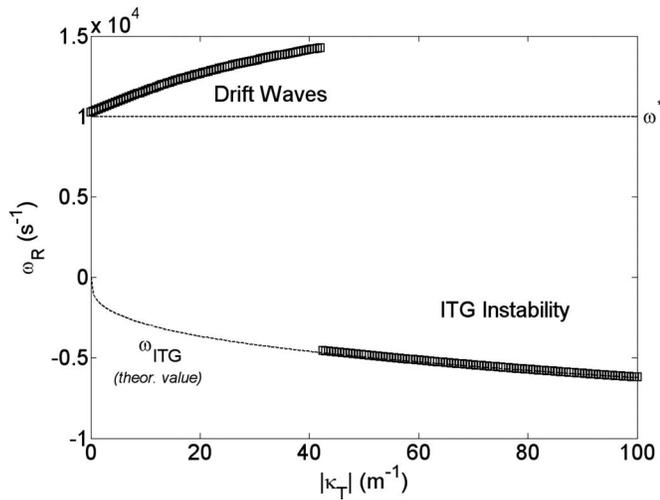
FIG. 9. Pulsation of the most unstable mode as a function of the parameter κ_T, with $\kappa_n = -10$ m^{-1}. ITG instability appears if κ_T exceeds a threshold value. Theoretical curves are shown for comparison.

For $|\kappa_T| > 42$ m^{-1}, ω_r becomes negative, meaning that the perturbation propagates in the ion diamagnetic drift direction as expected for ITG instabilities. Moreover, it is clear that ω_r given by the CGWB model is in good agreement with the theoretical prediction obtained within the framework of the fluid limit ($v_\varphi \gg v_{Ti}$) and with $\kappa_n = 0$:[22]

$$\omega_{\text{ITG}} = -\frac{1}{2}\left(\frac{k_\parallel^2 v_{T_i}^2 |\Omega_T^*|}{\tau}\right)^{1/3}, \tag{32}$$

where

$$\Omega_T^* = k_\theta \frac{K T_i}{qB} \kappa_T. \tag{33}$$

The very good agreement between these two curves allows us to conclude that ITG instabilities are actually observed. Nevertheless, the agreement between the two curves is less impressive if the ion temperature increases or if $v_{\parallel_0}$ changes, even if the agreement keeps being satisfactory enough.

Finally, these results show that for κ_T large enough, the ITG instability growth rate becomes greater than that of drift waves.

VIII. CONCLUSION

The water-bag model appears to be an interesting alternative to the usual fluid description for a laboratory magnetized plasma column. Interesting results have been obtained pointing to the ability of the collisional gyro-water-bag model to describe kinetic effects for drift waves and ITG instabilities. The analytical formulation of the linear dispersion equation as a summation over an assembly of oscillators provides a very clear description of the kinetic effects. Converting analytical problems into algebraic ones, without a loss of generality, represents one interesting property of the multi-water-bag model. As a direct consequence, the multi-water-bag problem converts the parallel velocity dependence into a set of hydrodynamic equations. Thus, the multiple wa-

ter bag offers an exact description of the plasma dynamics even with a small bag number, in the sense that the water-bag concept makes full use of the Liouville invariance in phase space. From a physical point of view, many interesting results can be obtained even with a small number of bags, basically $N=10$ or 20 bags, allowing much more analytical approaches bringing the link between the hydrodynamic description and the full Vlasov one.

In this paper, we have first presented the results obtained with the CGWB model in the case of the drift instability in a weakly ionized plasma in the collisional regime, with cold ions. Thus the CGWB model has been validated in the linear phase by comparing the calculated growth rates to a fluid model and experimental results in linear devices.

In order to excite ITG instabilities, the radial ion temperature gradient has to be increased. The CGWB model has been shown to be in good agreement with the ITG mode observed in the Columbia Linear Machine.

For larger ion temperatures we have studied the influence of kinetic effects on the collisional drift waves. We have shown that the linear growth rate given by a kinetic model is significantly lower than the one given by a fluid (or equivalent) model if the phase velocity of the instability is close to the ion thermal velocity.

One of the most important results of this paper was to prove that the CGWB model is able to study both collisional drift waves and ITG instability simultaneously. These instabilities depend strongly on the temperature gradient as measured by the κ_T parameter. It has been shown that as soon as the ITG instability appears this instability becomes dominant.

Of course, studying linear behavior is not enough to understand all the mechanisms involved and the processes responsible for the saturation of fluctuations. The results reported in this paper suggest that the CGWB model is able to depict the kinetic effects in the nonlinear regime at the numerical cost of a multifluid simulation. Actually, the water bag affords an exact reduction of the phase space dimension: no differential operation is carried out on the variable $v_\parallel$. Of course, the eliminated velocity reappears in the various bags j, but the multiple water bag offers an exact description of the plasma dynamics, while the full Vlasov equation needs to approximate a differential operator by some finite difference scheme. The use of an exact water-bag sampling should give better results than approximating differential operator. Very encouraging primary results have been obtained with a 3D code in cylindrical geometry and for electrons following the adiabatic law,[23] based on discontinuous-Galerkin type methods. A nonadiabatic collisional response of the electron will have to be introduced into the code for a CGWB simulation.

The next step will be to take under consideration the effects of the toroidal geometry (magnetic gradient and curvature drifts) which have been neglected in the present paper. Work is still in progress for a tokamak plasma.[34]

[1] A. M. Dimits, G. Bateman, M. A. Beer, B. I. Cohen, W. Dorland, G. W. Hammett, C. Kim, J. E. Kinsey, M. Kotschenreuther, A. H. Kritz, L. L. Lao, J. Mandrekas, W. M. Nevins, S. E. Parker, A. J. Redd, D. E. Shumaker, R. Sydora, and J. Weiland, Phys. Plasmas **7**, 969 (2000).
[2] X. Garbet, Plasma Phys. Controlled Fusion **43**, A251 (2001).

[3]P. C. Liewer, Nucl. Fusion **25**, 543 (1985).

[4]S. J. Zweben, J. A. Boedo, O. Grulke, C. Hidalgo, B. LaBombard, R. J. Maqueda, P. Scarin, and J. L. Terry, Plasma Phys. Controlled Fusion **49**, S1 (2007).

[5]L. Villard, S. J. Allfrey, A. Bottino, M. Brunetti, G. L. Falchetto, V. Grandgirard, R. Hatzky, J. Nührenberg, A. G. Peeters, O. Sauter, S. Sorge, and J. Vaclavik, Nucl. Fusion **44**, 172 (2004).

[6]T. Dannert and F. Jenko, Phys. Plasmas **12**, 072309 (2005).

[7]T. Pierre, G. Leclert, and F. Braun, Rev. Sci. Instrum. **58**, 6 (1987).

[8]M. Matsukuma, T. Pierre, A. Escarguel, D. Guyomarc'h, G. Leclert, F. Brochard, E. Gravier, and Y. Kawai, Phys. Lett. A **314**, 163 (2003).

[9]O. Grulke, T. Klinger, and A. Piel, Phys. Plasmas **6**, 788 (1999).

[10]C. Schröder, O. Grulke, T. Klinger, and V. Naulin, Phys. Plasmas **11**, 4249 (2004).

[11]E. Wallace, E. Thomas, A. Eadon, and J. Jackson, Rev. Sci. Instrum. **75**, 5160 (2004).

[12]R. G. Greaves, J. Chen, and A. K. Sen, Plasma Phys. Controlled Fusion **34**, 1253 (1992).

[13]R. F. Ellis and E. Marden-Marshall, Phys. Fluids **22**, 2137 (1979).

[14]E. Marden-Marshall, R. F. Ellis, and J. E. Walsh, Plasma Phys. Controlled Fusion **28**, 1461 (1986).

[15]V. Naulin, T. Windisch, and O. Grulke, Phys. Plasmas **15**, 012307 (2008).

[16]H. Sugama, T. H. Watanabe, and W. Horton, Phys. Plasmas **10**, 726 (2003).

[17]T. S. Hahm, Phys. Fluids **31**, 2670 (1988).

[18]V. Grandgirard, M. Brunetti, P. Bertrand, N. Besse, X. Garbet, P. Ghendrih, G. Manfredi, Y. Sarazin, O. Sauter, E. Sonnendrücker, J. Vaclavik, and L. Villard, J. Comput. Phys. **217**, 395 (2006).

[19]W. W. Lee, Phys. Fluids **26**, 556 (1983).

[20]A. Ghizzo, P. Bertrand, E. Fijalkow, M. R. Feix, and M. Shoucri, J. Comput. Phys. **108**, 105 (1993).

[21]X. Garbet, Y. Sarazin, V. Grandgirard, G. Dif-Pradalier, G. Darmet, Ph. Gendrih, P. Angelino, P. Bertrand, N. Besse, E. Gravier, P. Morel, E. Sonnendrücker, N. Crouseilles, J. M. Dischler, G. Latu, E. Violard, M. Brunetti, S. Brunner, X. Lapillone, T. Tran, L. Villard, and M. Boulet, Nucl. Fusion **47**, 1206 (2007).

[22]P. Morel, E. Gravier, N. Besse, R. Klein, A. Ghizzo, P. Bertrand, X. Garbet, P. Ghendrih, V. Grandgirard, and Y. Sarazin, Phys. Plasmas **14**, 112109 (2007).

[23]N. Besse, P. Bertrand, P. Morel, and E. Gravier, Phys. Rev. E **77**, 056410 (2008).

[24]F. R. Hansen, G. Knorr, J. P. Lynov, H. L. Pecseli, and J. Juul Rasmussen, Plasma Phys. Controlled Fusion **31**, 173 (1989).

[25]E. Gravier, X. Caron, G. Bonhomme, T. Pierre, and J. L. Briançon, Eur. Phys. J. D **8**, 451 (2000).

[26]C. Schröder, T. Klinger, D. Block, A. Piel, G. Bonhomme, and V. Naulin, Phys. Rev. Lett. **86**, 5711 (2001).

[27]E. Gravier, F. Brochard, G. Bonhomme, T. Pierre, and J. L. Briançon, Phys. Plasmas **11**, 529 (2004).

[28]F. Brochard, E. Gravier, and G. Bonhomme, Phys. Plasmas **12**, 062104 (2005).

[29]T. Klinger, A. Latten, A. Piel, G. Bonhomme, and T. Pierre, Plasma Phys. Controlled Fusion **39**, B145 (1997).

[30]G. Bachet, L. Chérigier, M. Carrère, and F. Doveil, Phys. Fluids B **5**, 3097 (1993).

[31]J. W. Connor and H. R. Wilson, Plasma Phys. Controlled Fusion **36**, 719 (1994).

[32]R. J. Goldston and P. H. Rutherford, *Introduction to Plasma Physics* (IOP, London, 1995), pp. 468–469.

[33]R. Scarmozzino, A. K. Sen, and G. A. Navratil, Phys. Rev. Lett. **57**, 1729 (1986).

[34]R. Klein, P. Morel, N. Besse, E. Gravier, and P. Bertrand, Proceedings of the 35th European Physical Society Conference on Plasma Physics (Hersonissos, Crete, Greece, June 9–13, 2008), p. P4.038.